Available online at www.sciencedirect.com
ScienceDirect
Journal of Power Sources 161 (2006) 1116–1125
JOURNAL OF POWER SOURCES
www.elsevier.com/locate/jpowsour

Removal of excess product water in a PEM fuel cell stack by vibrational and acoustical methods

Vikrant Palan, W. Steve Shepard Jr.*, Keith A. Williams

The University of Alabama, Department of Mechanical Engineering, 290 Hardaway Hall, Box 870276, Tuscaloosa, AL 35487, United States

Received 16 May 2006; received in revised form 24 May 2006; accepted 6 June 2006
Available online 28 July 2006

Abstract

The research presented here investigates the use of vibro-acoustic methods to improve the performance of a PEM fuel cell by enhancing water removal from the active reaction sites within the fuel cell. Removing the water increases the available reaction sites and thus increases the available power for a given operating condition. To examine the new water removal methods, first, the production of water in fuel cells and current water removal methods are reviewed. Then, the new methods are proposed that are based on structural and acoustical excitation of the stack. Specifically, the use of flexural waves, acoustic waves and surface waves to remove water from a fuel cell stack are examined. Analytical formulations are given in order to calculate the excitation frequency and amplitude required to move a droplet resting on a vibrating bipolar plate. Depending on the droplet radius and other parameters, it is estimated that a water droplet resting on a bipolar plate can be moved by structural displacement levels as low as 1 μm. The different approaches to droplet removal are compared in terms of the minimum vibration energy required per droplet. Water production in a commercial fuel cell stack is then estimated and used as a test case to compare the power required to effect removal of a certain number of droplets with the amount of power produced by the stack. It is shown that a water droplet clogging a plate channel may be moved with parasitic power requirements as low as 21 mW. For each method, the energy required to effect droplet removal is quite small, although among the three, the use of surface acoustic waves may be the best option in terms of minimal vibration energy and implementation feasibility.

Keywords: Water removal; Vibro-acoustic; Fuel cells; Surface waves; Performance enhancement

1. Introduction

The capital cost associated with fuel cell (FC) stacks is one of the major roadblocks to FC vehicle commercialization. The prices of prototype FC vehicles currently being introduced by various automakers are in the vicinity of US$ 1 million [1], a large part of which is due to the stack component and manufacturing costs. As the name implies, a fuel cell stack is a stack of individual fuel cells connected in series. The stacks are sized to obtain desired current and voltage (and hence power) outputs. One approach to reducing stack costs is, of course, to reduce the cost of the stack components, some of which are made with precious metals. Alternatively, if a fuel cell's performance could be improved, the stack size required for a given power output could be reduced, such that either fewer or smaller stack components could be used. In reality, contributions from both approaches will most likely be required. The focus of this paper is on the latter approach: improving the stack performance of a polymer electrolyte membrane (PEM) fuel cell stack. A PEM fuel cell is considered in this work, as it is one of the most preferred fuel cell designs in industrial use, due to its low operating temperature of approximately 80 °C [2]. The performance enhancement methods presented here are aimed at effectively removing the water produced as a result of chemical reactions in a PEM fuel cell, so that the available reaction sites will be increased. In the present study, the water of interest is in the form of condensation [3].

Water management is an important part of fuel cell operation. Water is the product of the electricity-producing chemical reactions inside the stack. In addition, the reactant gasses are often pre-humidified to improve their permeability through the electrolyte [4]. As a result, some of the humidification water is carried by the H^+ ions from the anode to the cathode through the electrolyte membrane in a process known as electro-osmotic

* Corresponding author. Tel.: +1 205 348 0048; fax: +1 205 348 6419.
E-mail address: sshepard@eng.ua.edu (W.S. Shepard Jr.).

0378-7753/$ – see front matter © 2006 Elsevier B.V. All rights reserved.
doi:10.1016/j.jpowsour.2006.06.021

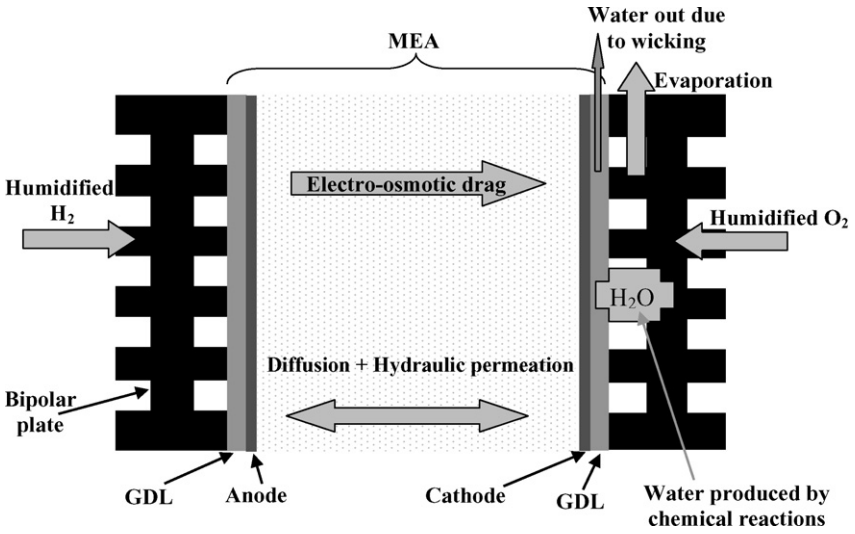

Fig. 1. Sources of water in fuel cells.

drag. Water can also diffuse from the cathode to the anode due to concentration and pressure gradients across the membrane electrode assembly (MEA). The locations and motions of water in a single fuel cell assembly are shown in Fig. 1.

While some water is beneficial to the stack performance, too much water can lead to a condition known as "flooding." Flooding in fuel cells is the condition when water clogs the channels of the bipolar plates and reduces the flow of reactant gases available for chemical reactions [5]. Moreover, flooding causes some of the water to block the reaction sites, thus affecting the rate of chemical reactions and, in turn, the FC efficiency.

As a result of the potential problems that result from excess water, various researchers have proposed methods to remove that excess water. These methods are based on water removal at either the anode or the cathode. A review of some of these methods is given in References [6,7]. One conventional water removal method is the use of capillary action or wicking, in the gas diffusion layer (GDL) [8]. The GDL is made out of a porous material and is located between the electrodes (anode and cathode) and the bipolar plates, as shown in Fig. 1. Water is drawn through the pores in this material by capillary action. Another method for water removal is to supply air (or oxygen) to the cathode at a rate significantly greater than the stoichiometric ratio. Typically, the oxygen excess ratio is 2.0; that is, oxygen is supplied at a rate twice as high as that necessary for the chemical reactions. One effect of the higher-than-stoichiometric ratio is that the excess gas flow can be used to "sweep out" the excess water on the cathode side of the cells [9]. Finally, the cell electrodes are often coated with a hydrophobic material in order to reduce the electrodes' affinity for water. These methods, although satisfactory, increase the fuel cell costs in terms of production and parasitic losses.

Another group of water removal methods generally referred to as "anode water removal" approaches, utilize gradient mechanisms: pressure [10], concentration [11] or temperature [12]. Water is driven from the cathode to the anode side of a given cell by creating at least one of those gradients across the MEA and bipolar plates. The main disadvantage of using this method is its detrimental effect on the ion transportation rate, as the water is diffusing through the membrane in a direction opposite to that of the H^+ ions traveling to the cathode. Also, the excess water accumulated on anode side, if not removed effectively, may reduce the amount of active reaction sites, thus affecting the rate of reaction and again reducing the system performance.

From the above discussion, it is evident that water management in fuel cells is an important engineering topic. The field of vibro-acoustics may offer non-conventional methods to realize water management in fuel cells. One approach to realizing water management in fuel cells that has already been investigated is the use of vibro-acoustics to achieve atomization of water droplets in the stack [13]. The present work examines an alternate approach: the bulk movement of water droplets within the fuel cells. Through vibro-acoustic means, it may be possible to move water droplets from the MEA to other locations such as drain ports. At the same time, this may be accomplished with no moving parts, should require very little power and would require minimal or even no changes in the fuel cell designs to enhance water movement in fuel cells. Furthermore, these methods may prove to be localizable, in that they can be implemented as needed at specific locations in the stack. For example, it may be sufficient to "turn on" vibro-acoustic actuators on only specific locations in the stack, such as clogged channels, while actuators at non-problem stack locations may be left "off" until needed. In that fashion, power will not be wasted by exciting non-problem areas of the stack. In contrast, water removal methods such as the use of significantly higher than stoichiometric air ratios are typically applied to the entire stack, rather than specific locations.

The next section presents a theoretical background for three vibro-acoustic methods which may be used to realize water droplet motion in a FC stack. These methods may potentially be applied to both the cathode and anode sides of individual fuel cells. The formulations are aimed at estimating the amplitude of vibration and consequently the minimum vibration energy required to move a droplet from one location to another in a bipolar plate channel. The three methods are differentiated in terms

of the mode of excitation used and include (a) generation of flexural waves in the bipolar plate, (b) use of acoustic waves in the flow and (c) use of localized surface waves in the bipolar plates. A general description for implementing each of these methods is given in the respective sub-section. The amount of energy per droplet is then calculated for each approach. An approach for estimating the number of water droplets that must be removed is then presented. That approach, although somewhat crude, provides a means for comparing the proposed methods in terms of the minimum overall vibration power required to effect water management in a given fuel cell stack and then comparing those values to the overall power produced by the fuel cell. A 1.2 kW fuel cell was considered for this comparison study. Finally, to provide perspective on the potential efficiency improvements that may be obtained a simple method to estimate the effect of flooding on overall FC performance is also given.

2. Theoretical background

The water management methods proposed in this work are intended to effect water removal by generating a force, F_{drop}, that is equal to the force of adhesion between the water and the supporting surface, F_{adh}. In equation form, the basis for water removal may be expressed as:

$$F_{drop} = F_{adh}. \tag{1}$$

The force of adhesion exerted on a droplet resting on a surface is given by [14,15]

$$F_{adh} = \sigma_w(1 + \cos\varphi_0)w, \tag{2}$$

where σ_w is the surface tension of the liquid droplet and w is the width of the droplet base, $w = 2R\sin(\varphi_0)$. Depending on the case examined, the supporting surface may be a membrane or a bipolar plate. Note that, in order to initiate droplet movement, F_{drop} must actually be greater than F_{adh}. However, once initiated, movement at a constant velocity requires only that Eq. (1) be satisfied and that equality will be taken as the benchmark for realizing water droplet removal.

A droplet resting on a surface is shown in Fig. 2. The assumption is that the droplet can be represented as the intersection of a sphere with a flat surface. The amount of water depends, on the contact angle φ_0 and the radius of the assumed sphere, R, both of which are shown in Fig. 2. The contact angle is a property of the surface on which the droplet rests. The bipolar plate is generally coated with a hydrophobic material such as Teflon to make water removal easier. The contact angle for a Teflonized surface is around 105° [16]. The percentage of the spherical volume that makes up the droplet increases with the droplet angle. For example, the extreme case of $\varphi_0 = 180°$ would imply a perfect sphere resting on top of a surface. The effective volume V_{eff} and surface area S_{eff} of the spherical droplet cap may be calculated using the relations [17]

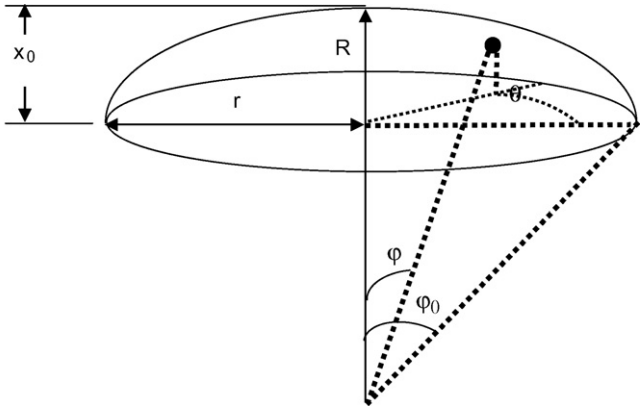

Fig. 2. Schematic of a water droplet cap.

$$V_{eff} = \left(\frac{\pi R^3}{3}\right)(1 - \cos\varphi_0)^2(2 + \cos\varphi_0), \tag{3}$$

and

$$S_{eff} = 2\pi R^2(1 - \cos\varphi_0). \tag{4}$$

In this work, the force F_{drop} required to induce droplet movement may be generated by:

(i) flexural plate waves;
(ii) acoustic waves;
(iii) surface waves.

The three methods discussed in this work differ in the way that the left hand side of Eq. (1) is calculated.

With this background and general set of equations, specific methods for water removal can be discussed. It should be noted here that some of the methods discussed below are based on the works of other researchers who have investigated the phenomena of droplet movement in general terms or for other applications. It is the goal of the present research to apply these studies to improve the product water removal in a FC system. This is done by tailoring some of the equations derived previously and by discussing implementation issues with regards to FC systems. The implementation of these methods may include issues such as the type of actuator used and its location in a FC stack. Also, the methods presented may potentially be used on both the bipolar plates as well as the membrane for water removal. Of course, additional information such as membrane materials and mechanical properties would be required to apply these methods to different components of the fuel cell stack. The analytical models presented here are discussed with respect to parameters such as droplet volume and excitation frequency to induce droplet movement on a bipolar plate.

2.1. Droplet movement using flexural plate waves (FPW)

The phenomena of droplet movement on plates have been presented by Scortesse et al. [18] and Biwersi et al. [19]. Those authors examined the generation of flexural waves on a plate by exciting the plate at frequencies in the range of the higher flexural modes. The flexural plate waves were used to impart energy to resting droplets and thus cause movement of the droplets in the direction of the traveling wave, as illustrated in Fig. 3. The main forces acting on a droplet due to flexural wave propagation are

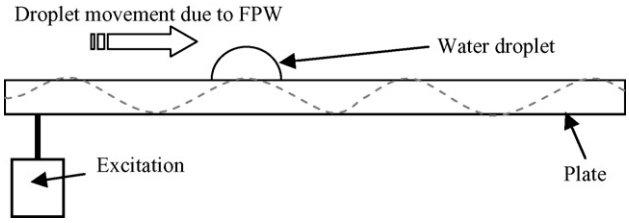

Fig. 3. Droplet movement on a plate by exciting flexural waves.

due to [20] the radiation pressure

$$P_{\mathrm{r}} = \frac{1}{4}\rho\omega^2 u^2 \left(2 + \frac{B}{A}\right) \sin^2(kx), \tag{5}$$

the capillary pressure

$$P_{\mathrm{c}} = \sigma \left(\frac{1}{R_x} + \frac{1}{R_y}\right), \tag{6}$$

and the hydrostatic pressure

$$P_{\mathrm{h}} = \rho g x, \tag{7}$$

where $k = 2\pi/\lambda$ is the wave-number, λ the corresponding wave length, ρ the liquid density and ω is the excitation frequency in rad s^{-1}. The parameters B and A are non-linear effect constants with the ratio $B/A = 5.2$ for liquids, u the vibration amplitude in meters and x is the direction of propagation of the flexural wave. The equation of capillary pressure is derived according to Laplace Law, explained in Reference [21]. In this equation, σ is the surface density of the liquid droplet and R_x and R_y are the radii of curvature on the horizontal surface of the plate in the respective directions. For a spherical droplet, $R_x = R_y = R$. Note that the equation for radiation pressure is time independent and second order. That equation is obtained by relating the pressure induced by the flexural waves at the solid–liquid interface, the ambient pressure and the droplet radius of curvature [20]. The harmonic term in the equation indicates the assumption of sinusoidal motion of the plate in flexure.

Of the three pressures listed above, the radiation pressure is observed to be the dominant contributor to the overall forces exerted on a resting droplet [22]. Defining the pressure amplitude P_{or} required to move a water droplet as:

$$P_{\mathrm{or}} = \frac{1}{4}\rho\omega^2 u^2 \left(2 + \frac{B}{A}\right). \tag{8}$$

The force F_X exerted on the droplet by radiation pressure can then be calculated by integrating the radiation pressure over the angles φ and θ, shown in Fig. 2, as:

$$F_X = \int_0^{\varphi_0} \int_0^{2\pi} P_{\mathrm{or}} \sin^2(kx) R^2 \sin^2\varphi \cos\vartheta \, \mathrm{d}\vartheta \, \mathrm{d}\varphi. \tag{9}$$

Equating this force to the adhesive force in Eq. (2) and solving for the pressure amplitude P_{or},

$$P_{\mathrm{or}} = \frac{\sigma_w(1 + \cos\varphi)w}{\int_0^{\varphi_0} \int_0^{2\pi} \sin^2(kx) R^2 \sin^2\varphi \cos\vartheta \, \mathrm{d}\vartheta \, \mathrm{d}\varphi}. \tag{10}$$

Given particular droplet parameters, Eq. (10) can be solved using the Matlab® function 'dblquad.' The resulting P_{or} can then be used with Eq. (8) to solve for the minimum vibration amplitude required to generate flexural waves that will cause droplet movement according to:

$$u = \sqrt{\frac{P_{\mathrm{or}}}{(1/4)\rho(2 + B/A)\omega^2}}. \tag{11}$$

The resultant vibration amplitudes for a few representative cases are presented in Section 3.1. Once the vibration amplitude u has been obtained, the corresponding vibration energy required for droplet movement using this method can also be calculated. This is given by [23]

$$E_{\mathrm{vib}} = \frac{1}{2}\rho_w U^2 V_{\mathrm{eff}}, \tag{12}$$

where U is the velocity amplitude of vibration, ρ_w the water density = 1000 kg m^{-3} and V_{eff} is the effective volume of the droplet given by Eq. (3).

A number of means are available for exciting a bipolar plate in order to generate the flexural waves required to effect droplet movement, including the use of electrodynamic shakers or piezoelectric (piezo) patches. Each method has its own advantages and disadvantages: a shaker is easily implemented, but may require excess space that is not available. Piezo patches are quite compact methods for applying forces to structures, but must be appropriately applied and attached in order to be effective. One other technology that is available is the piezoceramic inertial actuator [24]. That device is essentially a miniature shaker that uses piezoceramic rings to generate forces between an underlying structure and an inertial reaction mass.

No matter which method of excitation is used, modal analysis of the bipolar plates should be performed to determine resonant frequencies before selecting and placing actuators. The reason for this is that excitation of a plate at a resonant frequency is generally much more effective and efficient than at a non-resonant frequency. Exciting a lightly damped structure at resonance will result in significant displacements, even with relatively small force levels. In addition, modal analysis can be used to guide actuator placement and to avoid the problem of attaching actuators at node locations. This may be an interesting subject to pursue for further study.

Regardless of which excitation source is used, it may be attached to one or both of the end plates in a FC stack. End plates have channels cut only on one of its sides and they enclose all the other fuel cells in the stack. It should be ensured that the force exerted by the source is enough to achieve the required vibration levels for droplet movement in all the bipolar plates in the stack.

2.2. Droplet movement using modulated ultrasound

The next model presented is based on the analytical formulation given by Whitworth et al. [25]. Those authors demonstrated the movement and accumulation of polystyrene particles in water in the presence of high frequency, high intensity acoustic

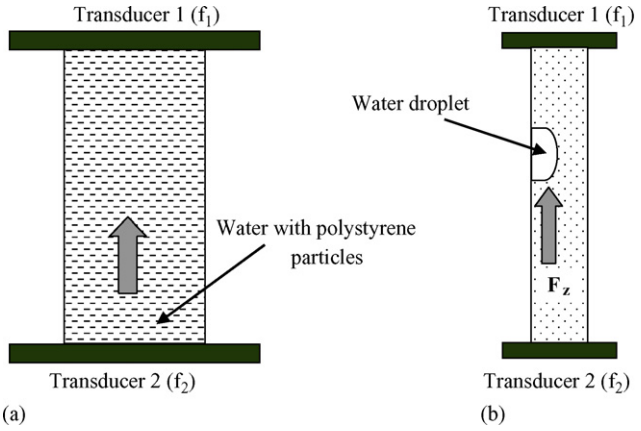

Fig. 4. Particle movement in a pseudo standing wave field; (a) polystyrene particles in water and (b) droplet movement in air in a bipolar plate channel.

waves. The authors observed that that movement was realized by generating a pseudo standing (slowly moving) wave field. A schematic of the experimental setup used to generate such a wave-field is provided in Fig. 4(a). Two piezo-actuators are located at opposite ends of a channel and are excited at slightly different frequencies, given by f_1 and f_2, where $f_1 > f_2$. The resulting acoustic force causes movement of the particles in the host medium from the low frequency side to the high frequency side. The maximum speed at which the particles move is given by:

$$v = \frac{\omega_1 - \omega_2}{k_1 + k_2}, \tag{13}$$

where ω_i and k_i refer to the angular frequency and wavenumber, respectively, that result from the excitation. The acoustic force acting on a particle or droplet in the presence of ultrasound is given by [25]

$$F_Z = VP^2 \left(\frac{k_1 + k_2}{8}\right) \left[B_r + \left(1 - \frac{\beta^*}{\beta}\right)\right], \tag{14}$$

where P is the acoustic pressure amplitude and V is the droplet volume. The terms β^* and β are the adiabatic compressibilities of the droplet and surrounding medium, respectively. Here, B_r is a quantity that results from the relative motion between the polystyrene particles and water. The value of B_r is estimated by using the excitation frequency and properties of the particle and the host such as densities and shear viscosity coefficients [26].

To implement this method in moving a droplet resting on a bipolar plate channel, consider a water droplet in air, instead of polystyrene particles in water. Piezoelectric speakers may be used as actuators in this case and are placed at the ends of the channels as shown in Fig. 4(b). The force F_z given by Eq. (14) and shown in the figure is required to overcome the adhesive forces that hold the droplet at a particular location. It is important to note that the actuators may be placed such that they do not cover the entire channel, so that the moving droplets will have space to exit the channel. Also, this will ensure that the actuators do not interfere with the reactant gas flows.

The force given in Eq. (14) is responsible for the movement of a particle or droplet in a medium. If this force is equated to the adhesive forces acting on a droplet, as given by Eq. (2), the minimum acoustic pressure required to move a droplet may be obtained. This acoustic pressure is thus given by:

$$P = \sqrt{\frac{\sigma(1 + \cos\varphi_0)w}{V[B + (1 - \beta^*/\beta)]((k_1 + k_2)/8)}}. \tag{15}$$

Once the acoustic pressure amplitude is known, the corresponding velocity amplitude of vibration U can be found using a plane-wave assumption

$$U = \frac{P}{\rho c}, \tag{16}$$

where ρ is the air density and c is the sound speed in air. The required vibration amplitude is estimated by taking Eq. (16) and dividing it by the angular frequency corresponding to f_1. These results are presented in Section 3.2. Once the vibration amplitude is known, the required vibration energy can be calculated as for the case of the standing waves using Eq. (12).

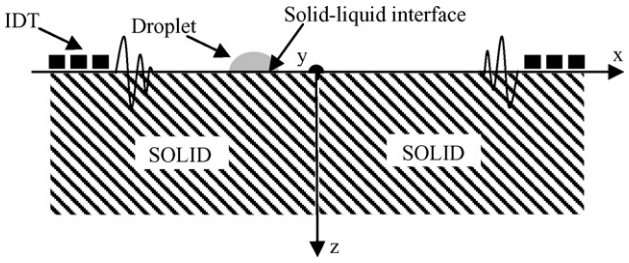

Fig. 5. Droplet movement on a SAW excited plate.

2.3. Droplet movement using surface acoustic waves (SAWs)

Surface waves, as their name suggests, are high-frequency waves localized at the surface of the material in which they are excited. It is because of this property that SAWs may be used to excite and move a small water droplet resting on a plate. There are various types of surface acoustic waves based on operating frequency, depth of penetration and sensitivity [27]. The most widely used surface wave-types are Rayleigh waves, Lamb waves, Love waves, Shear Horizontal (SH) waves and surface transfer waves, each of which is classified according to the specific type of acoustic wave used.

Rayleigh waves are one of the most widely used waves because of their high energy concentration on the surface [28] and better entrainment and directivity characteristics [29]. Moreover, Rayleigh waves are considered to be highly sensitive to surface mass loading [30]. This characteristic may be advantageous in moving small volumes of liquid resting on a surface excited by Rayleigh waves. The Rayleigh SAW radiates a wave component into a liquid droplet when the SAW propagation surface is in contact with that liquid. The wave component is normal to the plate surface, as shown in Fig. 5. That figure also shows a pair of inter-digital transducers (IDTs) that may be used to excite Rayleigh waves. IDTs are generally used to excite high-frequency, high-intensity surface waves [31]. As a first step to investigating the possibility of moving a droplet using Rayleigh

waves, it is important to estimate the force exerted by such a wave on the droplet and/or at the surface. The equation of radiation pressure generated by the Rayleigh waves was derived by Gol'dberg and Naugol'nykh [32]. The basic theory and wave equation for Rayleigh waves is given in References [33,34]. In one of his studies, Viktorov derived expressions for wave velocities at the solid–liquid interface [35]. That study assumed an infinite layer of fluid resting on the excited plate. Furthermore, that work was based on both analytical and experimental results. He observed that in case of Rayleigh waves, the wave velocities for the plate in the transverse direction are substantially higher than those in the longitudinal direction, which leads to higher energy transfer at the solid–liquid interface [36].

The approach used in the present study will involve estimating the vibration amplitudes required to move a droplet resting on a SAW-excited bipolar plate. To do this, it is first shown that the transverse component of displacement resulting from the excitation of a plate is dominant on the surface. It is this component that may be responsible for the droplet movement. Then, the equation for the pressure at the solid–liquid interface is derived. Using this pressure value, the corresponding force exerted on a liquid drop in the direction normal to the plate surface can b estimated. This force is then equated to the adhesive forces given by Eq. (2) in order to estimate the vibration amplitude required to move a droplet resting on a SAW excited plate.

To investigate the use of the SAW method in a FC system, a bipolar plate is considered with IDTs mounted at the ends. The voltage input to these IDTs will result in a proportional force exerted at the solid–liquid interface. Plane harmonic Rayleigh waves are shown propagating at the plate surface in Fig. 5. The components of longitudinal and transverse displacements in the x and z directions, U_R and W_R respectively, are given by [34,37]

$$U_R = Ak_R \left(e^{-q_R Z} - \frac{2q_R s_R}{k_R^2 + s_R^2} e^{-s_R Z} \right) \sin(k_R x - \omega t), \quad (17)$$

and

$$W_R = Aq_R \left(e^{-q_R Z} - \frac{2k_R^2}{k_R^2 + s_R^2} e^{-s_R Z} \right) \cos(k_R x - \omega t), \quad (18)$$

where A is a constant proportional to vibration amplitude; k_R is the Rayleigh wave number $= \omega/V_R$; ω is the excitation angular frequency; V_R the Rayleigh wave velocity; $q_R = k_R^2 - k_l^2$; $k_l = \omega/V_l$; $s_R = k_R^2 - k_t^2$; $k_t = \omega/V_t$. Here, V_l and V_t are the phase velocities of longitudinal and transverse waves respectively. V_l and V_t can be calculated based on the physical properties of the material

$$V_t = \sqrt{\mu/\rho}, \quad (19)$$

and

$$V_l = \sqrt{(\lambda + 2\mu)/\rho}, \quad (20)$$

where ρ is the material density and μ and λ are Lame constants that are determined by the material's Young's modulus, E and

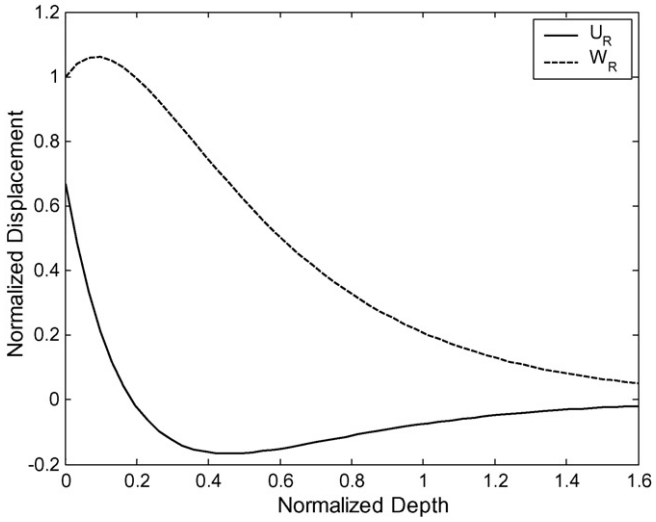

Fig. 6. Longitudinal (U_R) and transverse (W_R) displacement components.

Poisson's ratio, ν, according to:

$$\mu = \frac{E}{2(1+\nu)}, \quad (21)$$

and

$$\lambda = \frac{E\nu}{(1-2\nu)(1+\nu)}. \quad (22)$$

In the present study, the bipolar plates are considered to be made of steel with properties $\rho = 7700\,\mathrm{kg\,m^{-3}}$, $E = 195$ GPa and $\nu = 0.28$. Using those values with Eqs. (19)–(22) results in the phase velocities in longitudinal and transverse direction can be calculated to be $V_l = 5.7\mathrm{e}3\,\mathrm{m\,s^{-1}}$ and $V_t = 3.1\mathrm{e}3\,\mathrm{m\,s^{-1}}$, respectively. The Rayleigh wave velocity, V_R, is then calculated as a function of transverse wave velocity V_t and Poisson's ratio ν [38]:

$$V_R = \frac{0.87 + 1.12\nu}{1+\nu} V_t. \quad (23)$$

The magnitude of displacement amplitudes given by Eqs. (17) and (18) are plotted as a function of the normalized depth in Fig. 6 by using the parameters given above. This plot shows that the Rayleigh waves are concentrated at the surface and that they decay in the material as a function of the wavelength. The magnitudes are normalized with respect to the amplitudes at the surface ($z = 0$) and the depth is normalized with respect to Rayleigh wavelength λ_R. Note that the transverse component of displacement, W_R, is large at the surface as compared to the longitudinal component, U_R. As mentioned earlier, this characteristic may prove to be advantageous in exerting high force magnitudes at the interface. To estimate the force exerted on the droplet resting on the bipolar plate surface, the pressure generated by the Rayleigh waves is calculated first.

To calculate the pressure at the interface ($z = 0$), the pressure release boundary condition may be applied, which is given by:

$$\sigma_{zz} = 0, \quad (24)$$

where σ_{zz} is the normal stress component in the z direction, given by:

$$\sigma_{zz} = \lambda\left(\frac{\partial^2\phi}{\partial x^2} + \frac{\partial^2\phi}{\partial z^2}\right) + 2\mu\left(\frac{\partial^2\phi}{\partial z^2} + \frac{\partial^2\psi}{\partial x\,\partial z}\right), \tag{25}$$

where ψ and φ are the scalar and vector potentials, respectively at the interface given by:

$$\varphi = -A\,\mathrm{e}^{i(k_R x-\omega t)-q_R z}, \tag{26}$$

and

$$\psi = iA\frac{2k_R q_R}{k_R^2 + s_R^2}\mathrm{e}^{i(k_R x-\omega t)-s_R z}. \tag{27}$$

Substituting Eqs. (25), (26) and (27) in Eq. (24), the magnitude of the pressure at the interface, P_{int}, is obtained as

$$P_{int} = A\frac{-2\lambda k_l^2 k_R^2+\lambda k_l^2 k_t^2-4\mu k_R^4 + 2\mu k_R^2 k_t^2+4\mu k_R^2 q_R s_R}{2k_R^2 - k_t^2}\pi r^2. \tag{28}$$

The software package Maple® was used to evaluate Eqs. (24)–(28). The corresponding force exerted by this pressure at the interface can then be calculated by multiplying Eq. (28) by the contact area of the droplet. This force which is responsible for droplet movement was then equated to the adhesive forces on the droplet in Eq. (2) and solved for the constant A. The value of A was subsequently substituted into Eq. (18) to estimate the transverse vibration amplitudes required to move a droplet resting on a SAW-excited plate. The results for the estimated vibration amplitude are presented in a later section of this work. Once the transverse vibration amplitudes are known, the corresponding vibration energy required for droplet movement can again be calculated using Eq. (12).

Note that the techniques discussed above are for moving a single droplet of water. In an actual fuel cell stack, there may be several such droplets. A later section of this work discusses the method and assumptions made for estimating the number of droplets in a particular fuel cell. Once the number of droplets produced per minute is estimated, the three proposed methods are compared in terms of water removed and minimum vibration energy required to remove this water. Only water droplets at the cathode are considered in this study.

3. Results and discussion

The results for estimated vibration levels for each of the methods discussed above are presented in the following three sub-sections. The results are presented in terms of vibration amplitudes required to move a single droplet clogging or blocking the channels of a bipolar plate. An underlying assumption here is that the water droplets form in the channels and there is no water flow through the gas diffusion layer. This means that, for the purposes of this work, FC performance is characterized by the water flow in the channels. Also, it should be noted that the water droplets will continue to move across the plate surface, so long as the bipolar plate is excited. An estimate of droplet production in a specific fuel cell system is presented in Section 3.4 and is followed by the calculation of the minimum vibration power required to effect droplet movement for that level of droplet production.

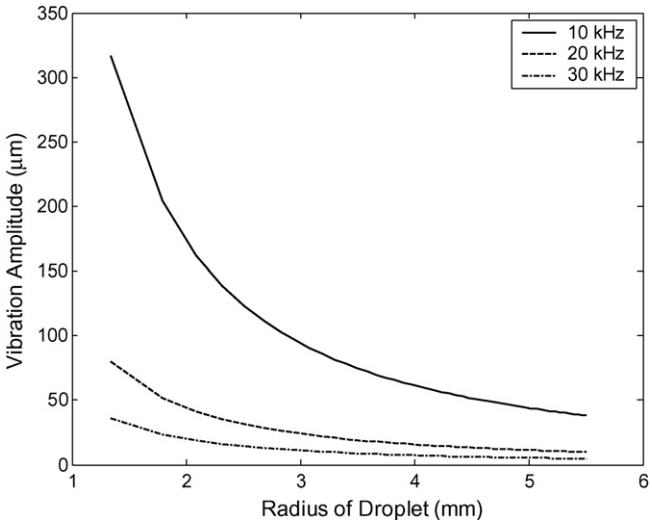

Fig. 7. Droplet movement requirements on vibration amplitude using flexural plate waves.

3.1. Method 1: water removal by flexural plate wave excitation (FPW)

The estimated flexural plate wave vibration amplitudes required to move a droplet on a vibrating plate are shown as a function of droplet size in Fig. 7 for three different excitation frequencies. The following numerical values are considered in plotting the results: speed of sound in water = 1481 m s^{-1}; x_0 (see Fig. 2) = 2.5 mm; surface tension for water–air system [8] = 72 mJ m^{-2}; B/A = 5.2 for liquids; density of water = ρ = 1000 kg m^{-3}.

Note first, from Fig. 7 that while the vibration amplitudes required to move the droplet are not substantial, the corresponding acceleration levels required will be sizeable because of the high excitation frequencies. An approximation of the acceleration levels may be obtained by squaring the excitation frequency (in rad s^{-1}) and multiplying it by the displacement amplitude. For example, given a 2 mm droplet radius, a vibration amplitude of 150 μm is required to effect droplet movement for an excitation frequency of 10 kHz. That corresponds to an acceleration amplitude of almost 60,000 g. Whether these high acceleration levels can be attained in a FC bipolar plate is a subject of future study. Specifically, the stresses in the plates must be estimated and compared to the yield stress for the particular plate material under consideration. Issues associated with fatigue must also be considered. Furthermore, it is possible that such high acceleration levels or even displacement levels may damage and/or delaminate the catalyst layer. Such problems will require consideration in future works. Even more important, experimental verification of these predictions is needed before it can be determined without a doubt that such an approach is even feasible. For the moment, however, the real point of interest is in determining the vibrational energy required to

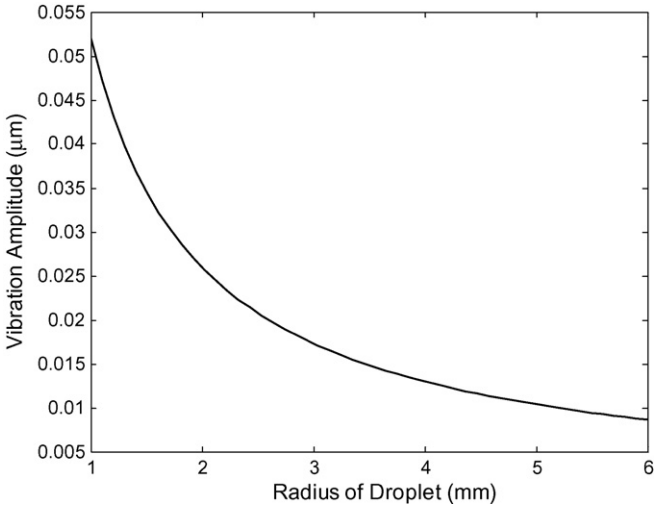

Fig. 8. Effect of droplet radius on vibration amplitude with the use of modulated ultrasound. Frequency difference between the two actuators is 200 Hz.

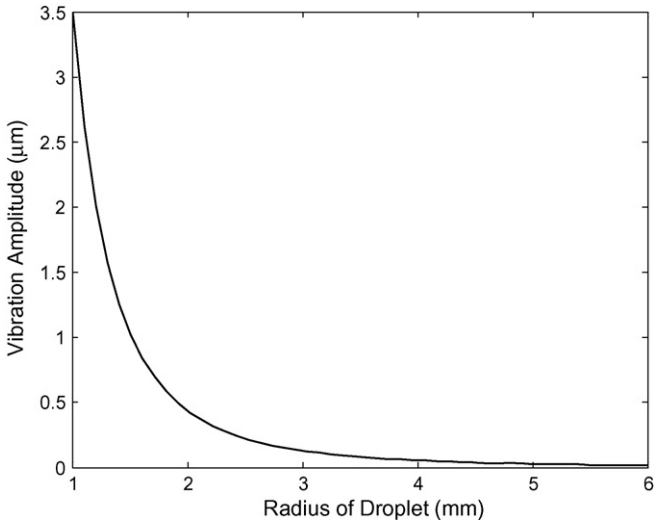

Fig. 9. Droplet movement requirements for vibration amplitude using Rayleigh waves approach.

effect droplet removal using this technique as will be presented shortly.

3.2. Method 2: droplet movement using modulated ultrasound

Fig. 8 shows the results obtained for required vibration amplitude to move a droplet using modulated ultrasound. The reference actuator was excited at a frequency (f_1) of 3 MHz. For this method to work, the excitation frequencies have to be very high. At lower frequencies, it was observed that substantially higher vibration amplitudes are required. In plotting various results in the figure, the following numerical values were considered: frequency difference $f_1 - f_2 = 200$ Hz; reference pressure $P_{\text{ref}} = 20\text{e}{-6}$ Pa; contact angle $\varphi_0 = 105°$; surface tension for water–air system $\sigma = 72$ mJ m^{-1}; adiabatic compressibility for water $\beta^* = 4.6\text{e}{-10}$ Pa^{-1}; adiabatic compressibility for air $\beta = 7.02\text{e}{-6}$ Pa^{-1}; density of water $\rho^* = 1000$ kg m^{-3}; density of air $\rho = 1.21$ kg m^{-3}; sound speed in air $c = 343$ m s^{-1}. The reason for selecting a frequency difference of 200 Hz was that the effect of frequency difference on vibration amplitude was found to be insignificant above 200 Hz.

As shown in Fig. 8, the required vibration amplitudes are very low as compared to the first method. It is clear from these observations that the applicability of this method would greatly depend on the ability and feasibility of inducing such high-frequency sound into the fuel cell system. Further work in the actuator and control mechanisms required to induce high frequency acoustic waves in plate channels may give additional insight into the viability of this method. Also, as with the first method, the analysis conducted here is also for moving a single drop.

3.3. Method 3: droplet movement using surface acoustic waves (SAW)

The vibration levels required for the use of surface acoustic waves are shown in Fig. 9. An excitation frequency of 10 kHz is considered for this particular case. Note that the vibration levels required for droplet movement using this method are much lower than those required for the use of flexural waves, while they are larger than those required for the use of ultra-sound waves. One of the reasons for smaller required displacements of the SAW-based approach, as compared to the flexural wave approach, is that the surface acoustic waves are localized to the surface of the solid, while in the case of the flexural waves, the entire structure is in motion.

3.4. Calculation of water droplet production

As mentioned in Section 2.1, the three methods for droplet movement presented here can be compared based on the minimum vibration power required to move a certain number of water drops per unit time. In order to calculate the vibration power levels, therefore, some information on the amount of water production in a fuel cell is necessary. To that end, water production in a commercially available 1.2 kW fuel cell system was considered. Although a chemical reaction balance and analysis would give the exact amount of water produced for this fuel cell [39], such a balance was not done here. Instead, data from the user's manual of the fuel cell system was used. According to that document, the water production on the cathode side of the bipolar plates in the fuel cell is 14.5 ml min^{-1}. For the purposes of the present discussion, it is assumed that water is produced and moves in droplet form, as opposed to continuous flow of water. Assuming 2 mm droplet radii, such that the effective volume of each droplet is 0.0231 ml, the number of droplets forming on the surface of the bipolar plates per minute, N_{drop}, is 628. That is, during every minute of operation, there are approximately 628 drops of water that may be responsible for flooding or blockage in the fuel cell stack under consideration. It is reasonable to expect that most of that water would naturally drain from the fuel cell. However, to provide a conservative estimate of the power required to effect droplet removal, it is assumed that all of that water will remain inside of the stack. Using that number

and the minimum vibration energy required to move a droplet by the three methods discussed earlier, the total vibration energy required to move all the droplets can be calculated. This comparison and analysis is presented in the examples discussed in the next section.

As mentioned earlier, the assumptions made in the estimation of number of droplets provide a sound platform for comparison of the above discussed water removal methods. It is important to remember that, as discussed in Section 1, the goal of realizing effective water removal is to improve the overall FC performance. The easiest method of quantifying potential performance improvements is to compare the predicted stack current output increases achieved when implementing each of the different water removal methods. The increased stack power can then be compared to the power required to effect the water removal. In the end, an experimental study will be required to truly validate the results. Such an approach is under consideration for a future work. At this preliminary stage, however, in order to determine if such an experimental study is warranted, a simpler approach will be taken. The assumption is made that the performance of a FC system is proportional to the total surface area of the active reaction sites [40]. It should be noted that this assumption was made to simplify the discussion and the resulting calculations. A more realistic assumption may be to consider just the channel area as opposed to the entire active reaction area. Such assumptions will be considered in future works. The fuel cell stack under consideration has 50 fuel cells connected in series and hence 50 active reaction areas. Considering each active area to be 50 mm × 50 mm, the total active reaction area will be 125e−3 m^2. The 628 droplets of 2 mm radius responsible for flooding would thus reduce the active reaction area by 7.9e−3 m^2. Therefore, the percent reduction, P_{red}, in performance may be estimated as $P_{red} = (7.9/125) \times 100 = 6.3\%$. Note that this is just the effect on performance every minute. If excess water accumulates over time, P_{red} may increase dramatically. Although it is understood that this is a rough estimation, the 6.3% reduction in performance demonstrates the effect that excess water can have on overall FC performance. Furthermore, that value provides a benchmark for comparing the different water removal methods; in order for any one of the methods to be a viable candidate for implementation in a fuel cell, the respective decrease in P_{red}, must outweigh the power requirements of that particular method.

3.5. Calculation of power requirements

The assumption is that 628 drops with 2 mm radii are formed every minute or a 2 mm droplet production of approximately 10.5 drops s^{-1}. Fig. 10 shows the minimum vibration energies required for the three proposed methods for different droplet radii. The variation in vibration levels for the three methods arises from the inherent difference in the way motion is generated by these methods. Methods 1–3, as discussed earlier, use flexural waves, acoustic waves and surface waves, respectively. Note that even though the required vibration amplitudes for droplet movement were lowest while using modulated ultrasound, the vibration energies are lowest for the SAW-based method. This is because of the high frequencies considered in the former case. From the figure, it appears that, theoretically, the use of surface waves may be the best option. Whether it is feasible to generate such waves in an actual fuel cell is a subject of further investigation.

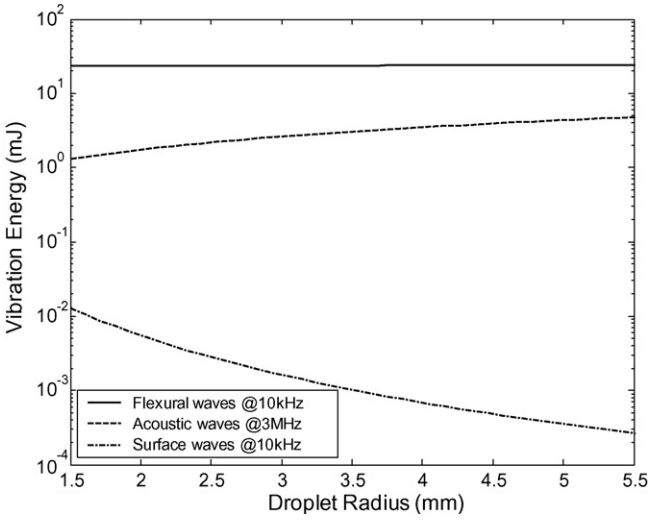

Fig. 10. Minimum vibration energy required to move 628 water droplets on a bipolar plate using flexural waves, acoustic wave and surface waves.

To examine the overall effect of the droplet removal methods on the fuel cell operation, the power to implement each method can be determined using the approximate droplet rate of 10.5 drops s^{-1}. For example, using flexural waves requires approximately 22 mJ $drop^{-1}$ or roughly 230 mW. Assuming a 2 mm droplet radius, the power requirements for the acoustic and surface wave approaches are 21 and 0.063 mW, respectively. Those power requirements should be compared against the rough estimate of a drop of approximately 6.3% or 75 W in a 1200 W system. Clearly, on paper, each of the three methods indicates a great deal of potential for improving the overall fuel cell system performance, with the surface acoustic waves offering the greatest potential gain. However, for each method, the power requirements are so small in comparison to the potential power improvements so as to be negligible. In that case, the choice of which water removal method to use should be based on implementation feasibility and the cost of the added sensors and actuators. As noted before, at this point, the analysis is entirely theoretical. The next step in this area is to implement different water removal methods on a functioning fuel cell and to obtain experimental validation of the predicted performance improvements.

4. Summary

The present study was motivated by the fact that fuel cell technology is still in its embryonic stages when it comes to its broad-based commercialization. The issue of performance enhancement is a subject of perennial research; hence the focal point of the present study. Higher performance results in smaller stack size and hence lower costs. Effective water removal is not only essential to the smooth running of fuel cells, but also

improves the performance if done effectively. To that end, fundamental methods were investigated that use waves such as flexural plate waves (FPW), acoustic waves and surface waves (SAW) to enhance the water removal process. Analytical models were developed to estimate the vibration levels and minimum vibration energies required at a particular frequency to move a water droplet of a particular size and volume on the surface of the bipolar plate. Specifically, it was shown that droplet movement can be induced by displacement amplitudes that are less than or equal to 1 μm. Moreover, it was found that excitation by surface waves provides the best option in terms of vibration energies required to move a droplet on the bipolar plate. In summary, it was theoretically shown that the proposed approaches, if implemented, may potentially result in better performance, hence reducing the overall FC stack cost. In the future, experimental or finite element modeling may be conducted to verify whether the required displacement and acceleration levels can be obtained in a fuel cell stack. Since the membranes between the plates are constructed out of a relatively soft material, it seems plausible that such vibration levels can be achieved.

References

[1] http://www.pbs.org/wgbh/nova/sciencenow/3210/01.html, 2005.
[2] G. Hoogers, Fuel Cell Technology Handbook, CRC Press, New York, 2003, pp. 1–4.
[3] P. Badrinarayanan, PEM fuel cell water and thermal management: a methodology to understand water and thermal management in an automotive fuel cell system, Master's Thesis, University of California, Davis, CA, 1999.
[4] F. Chen, Y.-G. Su, C.-Y. Soong, W.-M. Yan, H.-S. Chu, J. Electroanal. Chem. 566 (2004) 85–93.
[5] D. P. Wilkison, H. H. Voss, D. S. Watkins, K. Prater, B., Solid polymer fuel cell systems incorporating water removal at the anode, US Patent number 5,366,818 (1994).
[6] D.P. Wilkison, H.H. Voss, B. K. Prater, J. Power Sources 49 (1994) 117–127.
[7] B. K. Prater, J. Power Sources 51 (1994) 129–144.
[8] U. Pasaogullari, C.Y. Wang, J. Electrochem. Soc. 151 (2004) A399–A406.
[9] K. Tuber, D. Pocza, C. Hebling, J. Power Sources 124 (2003) 403–414.
[10] H.H. Voss, D.P. Wilkison, D.S. Watkins, Method and apparatus for removing water from electrochemical fuel cells, US Patent number 5,260,143 (1993).
[11] H.H. Voss, D.P. Wilkison, P.G. Pickup, Electrochem. Acta 40 (1995) 321–328.
[12] H.H. Voss, D.P. Wilkison, D.S. Watkins, Method and apparatus for removing water from electrochemical fuel cells by controlling the temperature and pressure of the reactant streams, US Patent number 5,441,819 (1995).
[13] V. Palan, W.S. Shepard, Water removal in a fuel cell stack by droplet atomization using structural and acoustic excitation, J. Power Sources 159 (2006) 1061–1070.
[14] J. Israelachvili, Intermolecular and Surface Forces, Academic Press, New York, 1991.
[15] A. Torkkeli, J. Saarilahti, A. Haara, Electrostatic transportation of water droplets on superhydrophobic surfaces, in: 14th IEEE International Conference on Micro Electro Mechanical Systems (MEMS 2001), Interlaken, 2001, pp. 475–478.
[16] M. Washizu, IEEE Trans. Ind. Appl. 34 (1998) 732–737.
[17] R.J. Hunter, Foundations of Colloid Science, Oxford University Press, New York, 2001, pp. 100–112.
[18] J. Scortesse, J.F. Manceau, F. Bastien, J. Sound Vib. 254 (2002) 927–938.
[19] S. Biwersi, J.F. Manceau, F. Bastien, J. Acoustical Soc. Am. 107 (2000) 661–664.
[20] S. Alzuaga, J.F. Manceau, S. Ballandras, F. Bastien, Displacement of droplets on a surface using ultrasonic vibration, in: World Congress on Ultrasonics, Paris, 2003, pp. 951–954.
[21] J. Lyklema, Introduction Fundamentals of Interface and Colloid Science, vol. 1, Academic Press, New York, 1993, pp. 294.
[22] L.V. King, R. Soc. Lond. Sect. A: Math. Phys. Sci. CXLVII (1934) 212–241.
[23] L.E. Kinsler, A.R. Frey, A.B. Coppens, J.V. Sanders, Energy of Vibration, in: Fundamentals of Acoustics, fourth ed., John Wiley & Sons, Inc., New York, 2000, p. 5.
[24] C.L. Davis, G.A. Lesieutre, An actively tuned solid-state vibration absorber using capacitive shunting of piezoelectric stiffness, J. Sound Vib. 232 (3) (2000) 601–617.
[25] G. Whitworth, M.A. Grundy, W.T. Coakley, Ultrasonics 29 (1991) 439–444.
[26] G. Whitworth, Particle movements in a rotating ultrasonic waveguide, PhD Thesis, Interdisciplinary Program in Biophysics, University of Virginia, 1989.
[27] M.J. Vellekoop, Ultrasonics 36 (1998) 7–14.
[28] R. Stoneley, Proc. R. Soc. Lond. 106, 1924, pp. 416–428.
[29] I.A. Viktorov, O.M. Zubova, Soviet Phys. Acoustics 9 (1963) 138–141.
[30] M.I. Newton, M.K. Banerjee, T.K.H. Starke, S.M. Rowan, G. McHale, Sens. Actuators 76 (1999) 89–92.
[31] M.G. Pollack, R.B. Fair, Appl. Phys. Lett. 77 (2000) 1725–1726.
[32] Z.A. Gol'dberg, K.A. Naugol'nykh, Soviet Phys. Acoustics 9 (1963) 22–24.
[33] I.A. Viktorov, Rayleigh and Lamb Waves: Physical Theory and Applications, Plenum Press, New York, 1967.
[34] E.A. Ash, E.G.S. Paige (Eds.), Rayleigh-Wave Theory and Application, Springer-Verlag, New York, NY, 1985.
[35] I.A. Viktorov, E.K. Grishchenko, T.M. Kaekina, Soviet Phys. Acoustics 9 (1963) 131–137.
[36] K. Miyamoto, S. Nagatomo, Y. Matsui, S. Shiokawa, Jpn. J. Appl. Phys. 41 (2002) 3465–3468.
[37] D.P. Morgan, Surface-Wave Devices for Signal Processing, Elsevier Science Publishers, Amsterdam, The Netherlands, 1985.
[38] I.A. Viktorov, Rayleigh and Lamb Waves: Physical Theory and Applications, Plenum Press, New York, 1967.
[39] M.C. Kimble, N.E. Vanderborgh, Reactant gas flow fields in advanced PEM fuel cell designs, in: Proceedings of the 27th Intersociety Energy Conversion Engineering Conference, vol. 3, Society of Automotive Engineers, Inc., San Diego, CA, 1992, pp. 3.413–413.417.
[40] J. Larminie, A. Dicks, Introduction, in: Fuel Cell Systems Explained, John Wiley & Sons Ltd., West Sussex, England, 2003, pp. 2–6.